# Multisensory integration operates on correlated input from unimodal transients channels

**Short title:** Multisensory integration and unimodal transient channels

**Authors:** Cesare V. Parise[1,2] & Marc O. Ernst[3,2]

**Affiliations:** [1] Department of Psychology, University of Liverpool (UK);
[2] Cognitive Neuroscience Department, University of Bielefeld (DE);
[3] Department of Psychology, University of Ulm (DE)

**Abstract**

Audiovisual information reaches the brain via both sustained and transient input channels, representing signals' intensity over time or changes thereof, respectively. To date, it is unclear to what extent transient and sustained input channels contribute to the combined percept obtained through multisensory integration. Based on the results of two novel psychophysical experiments, here we demonstrate the importance of the transient (instead of the sustained) channel for the integration of audiovisual signals. To account for the present results, we developed a biologically-inspired, general-purpose model for multisensory integration, the Multisensory Correlation Detectors, which combines correlated input from unimodal transient channels. Besides accounting for the results of our psychophysical experiments, this model could quantitatively replicate several recent findings in multisensory research, as tested against a large collection of published datasets. In particular, the model could simultaneously account for the perceived timing of audiovisual events, multisensory facilitation in detection tasks, causality judgments, and optimal integration. All-in-all, this study demonstrates that several phenomena in multisensory research that were previously considered unrelated, all stem from the integration of correlated input from unimodal transient channels.

## Introduction

Audiovisual stimuli naturally unfold over time, and their structures alternate intervals during which the signals remain relatively constant (such as the steady luminance of a light bulb) to sudden moments of change (when the bulb lights up). To efficiently process the temporal structure of incoming signals, the sensory systems of mammals (and other animal classes) rely on separate channels, encoding stimulus intensity through either sustained or transient responses [1–6]. Sustained channels respond with constant neural firing to static input intensity, whereas transient channels respond with increased firing to any variations in input intensity (i.e., both increments and decrements, Figure 1A). On a functional level, the response of sustained and transient channels represents distinct dynamic stimulus information. Specifically, sustained responses represent the intensity of the stimulus, while transient responses represent changes in stimulus intensity. In terms of frequency response, sustained channels can be characterised as low-pass temporal filters (Equation 10), highlighting the low-frequency signal components. Transient channels, on the other hand, have a higher spectral tuning and can be characterised as band-pass temporal filters (Equation 1), signalling events or moments of stimulus change [7].

Changing information over time is also critical for multisensory perception [8]: when two signals from different modalities are caused by the same underlying event, they usually covary over time (like firecrackers' pops and blazes). A growing body of literature has now investigated human sensitivity and adaptation to temporal lags across the senses [9], and it is well established that both multisensory illusions [10–12] and Bayesian-optimal cue integration (e.g., [13]) critically depend on synchrony and temporal correlation across the senses. However, multisensory integration does not operate on the raw sensory signals; these are systematically transformed during transduction and early neural processing. Therefore to understand multisensory integration, it is critical to figure out how unisensory signals are processed before feeding into the integration stage. Surprisingly, this fundamental question has received little attention in multisensory research.

Current evidence, however, suggests a prominence of transient channels in the percept resulting from multisensory integration. For example, Andersen and Mamassian [14] found that task-irrelevant increments or decrements in sound intensity equally facilitated the detection of both increments and decrements in the lightness of a visual display. Critically, such an effect only occurred when changes in the two modalities occurred in approximate

temporal synchrony. Based on this independence of polarity of this crossmodal facilitation, where intensity increments and decrements produced similar perceptual benefits, the authors concluded that audiovisual integration relies primarily on unsigned transient stimulus information. The role of transient channels in audiovisual perception is further supported by fMRI evidence: Werner and Noppeney [15] found that audiovisual interactions in the human brain only occurred during stimulus transitions, and demonstrated that transient onset and offset responses could be dissociated both anatomically and functionally (see also, [16]). While these studies demonstrate the dominance of transient over sustained temporal channels in e.g. detection tasks as studied by Andersen and Mamassian [14], or the pattern of neural responses during passive observation of audiovisual stimuli as in Herdener et al [16], to date, it is still unknown to what extent transient and sustained channels affect the perceived timing of audiovisual events – such as the subjective synchrony of visual and auditory signals, which is arguably the primary determinant of multisensory integration.

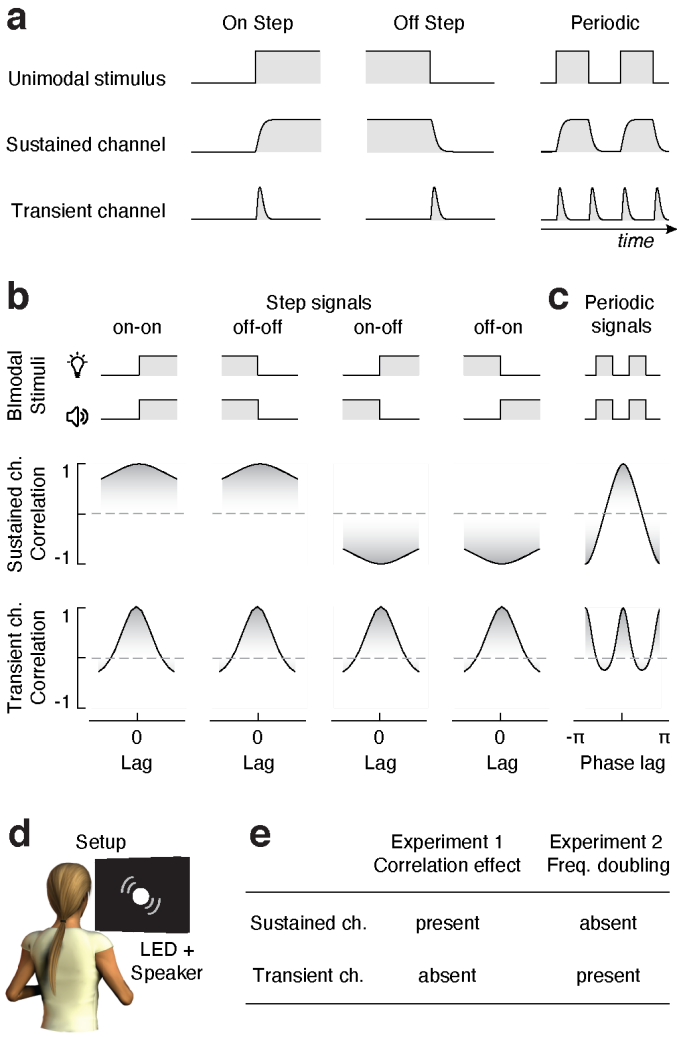


***Figure 1. Sustained vs transient channels. A.*** *Responses of sustained and transient channels to onset and offset step stimuli, and periodic signals comprising sequences of onsets and offsets. Note that while the sustained channels closely follow the intensity profile of the input stimuli, transient channels only respond to changes in stimulus intensity, and such a response is always positive, irrespective of whether stimulus intensity increases or decreases. Therefore, when presented with periodic signals, while the sustained channels respond at the same frequency as the input stimulus (frequency following), transient channels respond at a frequency that is twice that of the input (frequency doubling).* ***B.*** *Synchrony as measured from cross-correlation between pairs of step stimuli, as seen through sustained (top) and transient (bottom) channels (transient and sustained channels are simulated using Equations 1 and 10, respectively). Note how synchrony (i.e, correlation) for sustained channels peaks at zero lag when the intensity of the input stimuli changes in the same direction, whereas it is minimal at zero lag when the steps have opposite polarities (negatively correlated stimuli). Conversely, being insensitive to the polarity of intensity changes, synchrony for*

*transient channels always peaks at zero lag.* ***C.*** *Synchrony (i.e., cross-correlation) of periodic onsets and offset stimuli as seen from sustained and transient channels. While synchrony peaks once (at zero phase shift) for sustained channels, it peaks twice for transient channels (at zero and pi radians phase shift), as a consequence of its frequency doubling response characteristic.* ***D.*** *Experimental apparatus: participants sat in front of a black cardboard panel with a circular opening, through which audiovisual stimuli were delivered by a white LED and a loudspeaker.* ***E.*** *Predicted effects of Experiments 1 and 2 depending on whether audiovisual integration relies on transient or sustained input channels. The presence of the effects of interest in both experiments or the lack thereof indicates an inconclusive result, not interpretable in the light of our hypotheses.*

To understand the effect of transient versus sustained channels in multisensory perception, we must first focus on the difference between their unimodal responses. For that, we can consider stimuli consisting of steps in stimulus intensity (e.g.[14]. A schematic representation is shown in Figure 1A: while onset and offset step stimuli trigger identical unsigned transient responses, sustained responses differ across conditions. That is, given that sustained channels represent the magnitude of the stimulus, responses to onset and offset stimuli are negatively correlated. In signal processing, Pearson correlation is commonly used to assess the synchrony of two related signals, with a higher correlation representing higher synchrony (and similarity) [17]. Therefore, we can hypothesise that if multisensory time perception relies on sustained input channels, positively correlated audiovisual stimuli (e.g., onset or offset stimuli in both modalities) should be perceived as more synchronous than negatively correlated stimuli (i.e., onset in one modality, offset in the other). Conversely, if audiovisual synchrony relies on unsigned transients, positively and negatively correlated stimuli should appear equally synchronous (Figure 1B).

This hypothesis will be tested in Experiment 1, where systematic differences in perceived synchrony based on whether audiovisual signals are positively or negatively correlated, would provide evidence for a dominant role of sustained input channels in audiovisual temporal processing. A lack of systematic differences driven by stimulus correlation, however, would not necessarily imply a transient nature of audiovisual temporal processing: this would require additional evidence from an inverse experiment, one in which the transient hypothesis predicts an effect that the sustained hypothesis does not (Figure 1E). For that, we can consider audiovisual stimuli consisting of periodic onsets and offsets (e.g., square-wave amplitude modulation, see Figure 1C). While sustained channels respond at the same rate as the input, transient responses have a rate double that of the input signals. This phenomenon, known as

frequency doubling, is commonly considered a hallmark of the contribution of transient channels in sensory neuroscience (e.g.,[2]).

Frequency doubling, therefore, is a handle to assess the contribution of transient and sustained channels in audiovisual perception. Consider audiovisual stimuli defined by square-wave amplitude modulations with a parametric manipulation of crossmodal phase shift (Figure 1C). If audiovisual temporal integration relies on the correlation between sustained input channels, we can predict perceived audiovisual synchrony (i.e., correlation, [17]) to peak just once: at zero phase shifts. Conversely, if multisensory temporal integration relies on transient channels, perceived audiovisual synchrony should peak twice: at zero and 180deg. phase lag (Figure 1C). Such a frequency doubling phenomenon can be easily assessed psychophysically, by measuring reported simultaneity as a function of audiovisual lags. Therefore, in a second psychophysical study, we rely on frequency doubling in audiovisual synchrony perception to assess whether multisensory integration relies on transient or sustained input channels.

**Experiment 1: Step stimuli**

To probe the effect of the correlation between unimodal step stimuli on the perceived timing of audiovisual events, eight participants (age range 22–35 years, four females) observed audiovisual signals consisting of lightness and acoustic intensity increments (on-step) and decrements (off-step). On-steps and off-steps were paired in all possible combinations, giving rise to four experimental conditions (both modalities on, both off, vision on with audio off, and vision off with audio on, see Figure 1B). The lag between visual and acoustic step events was parametrically manipulated using the method of constant stimuli (15 steps, between -0.4 and 0.4s). After the stimulus presentation, participants performed a temporal order judgment (TOJ, which event came first, sound or light?) or a simultaneity judgment (SJ, were the stimuli synchronous or not?). TOJ and SJ tasks were run in different sessions occurring on different days. Although our original hypotheses (see, Figure 1B-E) do not make specific predictions for the TOJ task, for completeness we run such an experiment anyway, as its inclusion provides a more stringent test for our model (see “Modelling” section).

The audiovisual display used to deliver the stimuli consisted of a white LED in an on- (high-luminance) and off-state (low-luminance), and acoustic white noise, also in either on-

(quiet) or off-state (loud). Sounds came from a speaker located behind the LED, and both the speaker and the LED were controlled using an audio interface to minimize system delay (Figure 1D)(see [18]. A white, sound transparent cloth was placed in front of the LED so that when the light was on, participants saw a white disk of 13° in diameter. Overall, each participant provided 600 responses in the TOJ task (15 lags, 10 repetitions, and 4 conditions) and additional 600 responses in the SJ task (again, 15 lags, 10 repetitions, and 4 conditions). The experiment was run in a dark, sound-attenuated booth, and the position of participants' heads was controlled using a chin- and a headrest. Participants were paid 8 Euro/hour. The experimental procedure was approved by the Ethics committee of the University of Bielefeld and was conducted in accordance with the declaration of Helsinki.

**Results.** To assess whether different combinations of on-step and off-step stimuli (and correlation thereof) elicit measurable psychophysical effects, we estimated both the point and the window of subjective simultaneity (PSS and WSS, that is, the delay at which audiovisual stimuli appear simultaneous, and the width of the window of simultaneity). For that, we fitted psychometric curves to both TOJ and SJ data, independently for each condition. Specifically, following standard procedures [19], TOJs were statistically modelled as cumulative Gaussians, with 4 free parameters (intercept, slope, and two asymptotes, Figure 2A). The PSS was calculated as the lag at which TOJs were at chance level, whereas the window of simultaneity (WSS) was calculated as the half-difference between the lags eliciting 0.75 and 0.25 probability of audio-first responses. The SJs data, instead, were modelled as the difference of two cumulative Gaussians [20], leading to asymmetric bell-shaped psychometric functions (Figure 2B). The PSS was calculated as the lag at which perceived simultaneity was maximal, whereas the window of simultaneity was calculated as the half-width at half-maximum. Results are summarized in Figure 2C-D (see Supplementary Figure S1 for individual data, and Supplementary Information for a correlation analysis of the PSS and WSS measured from TOJs vs SJs).

To assess whether the four experimental conditions differ in the point and window of perceived simultaneity (PSS & WSS), we run non-parametric Friedman tests, with Bonferroni correction for multiple testing. Neither PSS nor WSS statistically differed across conditions, and this was true for both the TOJ and SJ data. Results are summarized in Table S2.

**Discussion.** The lack of a difference across conditions found in Experiment 1 implies that the on-step and off-step stimuli induced similar perceptual responses. Based on our original

hypothesis, the present results argue against the dominance of sustained input channels in the perception of audiovisual events, as the synchrony (i.e., Pearson correlation, [17]) of sustained signals, would otherwise have been affected by the crossmodal combination of on-step and off-step stimuli. As previously mentioned, while a lack of difference across conditions in Experiment 1 is necessary to infer a dominance of transient channels in audiovisual time perception, this evidence is not sufficient on its own. For that, we would need additional evidence in the form of the presence of systematic effects, which are predicted from the operating principles of the transient channels, but not for sustained ones. Experiment 2 was designed to fulfil such a requirement, as it predicts a frequency-doubling effect in perceived synchrony for transient but not for sustained input channels.

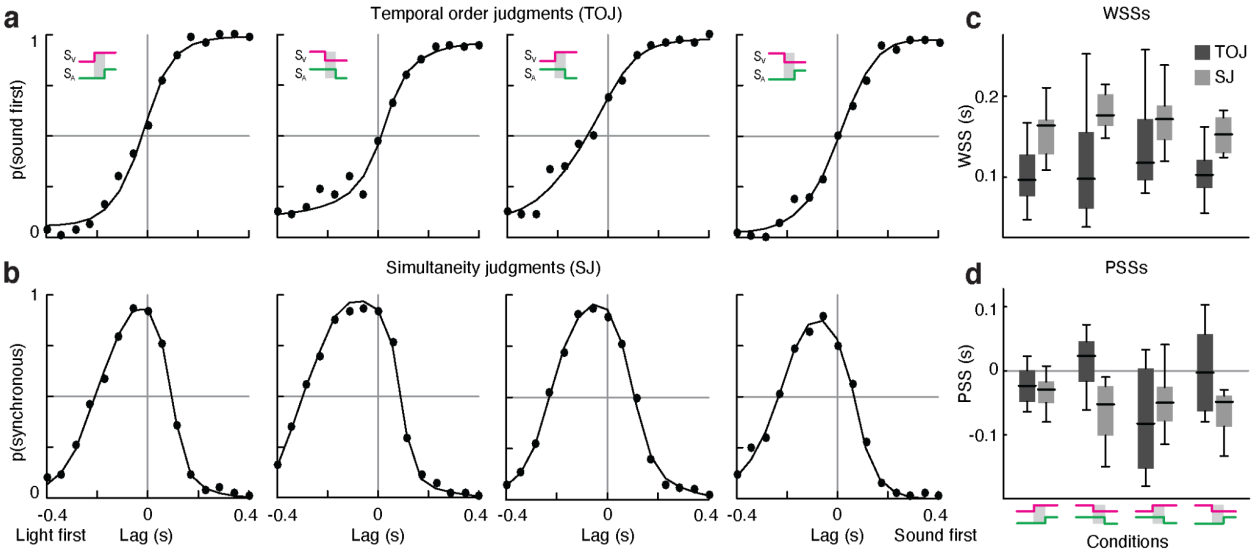


***Figure 2. Experiment 1, results**. **A.** Responses in the TOJ task and psychometric fits (averaged across participants) for the four experimental conditions. **B.** Responses in the SJ task and psychometric fits (averaged across participants) for the four experimental conditions. Each dot in panels A and B corresponds to 80 trials. **C.** Window of subjective simultaneity for each condition and task. **D.** Point of subjective simultaneity for each condition and task.*

**Experiment 2: Periodic stimuli.**

Participants observed a periodic audiovisual stimulus consisting of a square-waved intensity envelope and performed a force-choice simultaneity judgment task. The carrier visual and auditory stimuli consisted of pink noise, delivered by a speaker and an LED (Figure 1D), which were switched on and off periodically in a square-wave fashion with a period of 2 s for a total duration of 6 s (so that three full audiovisual cycles were presented on

each trial, Figure 3A). To prevent participants from just focusing on the start and endpoint of the signals, during the intertrial interval, the visual and auditory stimuli were set to a pedestal intensity level, so that during the trial, the square wave modulation was gradually ramped on and off, following a raised cosine profile with a duration of 6 s (Figure 3A).

The lag across the sensory signals consisted of relative phase shifts of the two square waves, while the raised cosine window remained constant (and synchronous across the senses). Audiovisual phase shift was manipulated according to the method of constant stimuli, and a full cycle was sampled in 40 steps. Each lag was presented 15 times to yield a total of 600 trials per participant. Besides the relative phase shifts across the multisensory signals, also the phase offset of the stimulus as a whole varied pseudorandomly across trials (spanning a full period sampled in 15 steps, one per repetition). Therefore, each time a given lag (phase shift) was tested; also the phase offset of the signals changed. Given that we expect the frequency doubling effect to be strong in size (i.e., synchrony at pi-phase shift should approach zero under the sustained hypothesis, and one under the transient hypothesis), and that we collected a large number of responses (n=600 per observer), a pool of five participants (age range 25–35 years, three females) was large enough to reliably assess its presence or lack thereof. Participants were paid 8 Euro/hour, and the experimental procedure was approved by the Ethics committee of the University of Bielefeld and was conducted in accordance with the declaration of Helsinki.

**Results.** Due to the periodic nature of the stimuli and hence of the experimental manipulation of lag, the resulting psychometric functions are also expected to be periodic, with an alternation of phase shifts yielding higher and lower reported synchrony. In this context, the evidence of frequency doubling can be measured from the number of oscillations in perceived simultaneity for a full cycle of phase shifts between the audiovisual stimuli.

Given the periodicity of the stimuli, it is natural to analyze the psychometric functions in the frequency domain. Therefore, to get a non-parametric and assumption-free estimate of the frequency of oscillations in the data, we ran a Fourier analysis on the empirical psychometric curves. If human responses are driven by transient input channels, we predict a peak at 2 cycles-per-period (cpp. i.e., frequency doubling), otherwise, there should be a peak at 1 cpp. The power spectrum of the psychometric functions shows a sharp peak at a frequency of 2 cpp in all observers, thereby indicating the presence of the hypothesized frequency doubling effect (Figure 3B and Supplementary Figure S2). To assess whether the amplitude at 1 and 2

cpp are statistically different at the individual observer level, we used a bootstrap procedure to estimate the confidence intervals of the response spectrum. For that, we used the binomial distribution and simulated 50000 psychometric functions, on which we performed a frequency analysis to obtain the 99% confidence intervals of the amplitudes. The results for both the aggregate observer and the individual data ) show a clear separation between the confidence intervals of the amplitude at the frequencies of 1 and 2 cpp and demonstrate that the 2 cpp is indeed the dominant frequency, whereas the amplitude at 1 cpp is close to 0 and it is no different from the background noise (i.e., higher harmonics; see Figure 3B, and Supplementary Figure S2).

Given that the frequency analyses revealed a 2 cpp peak for all participants, we used this information to fit a sinusoidal psychometric function to the psychophysical data. Under the assumption of late Gaussian noise, the psychometric function can be written as:

$$p(synch|\phi) = normcdf(\alpha + \beta \cdot sin(f\phi + \theta)),$$

where the parameter α is the bias term, β the sensitivity, ϕ the phase-lag (range=[0, 2π]), f the frequency of oscillations, and θ is the phase offset (this shifts peak synchrony toward either positive or negative phases). Based on the Fourier analyses, we fixed the frequency ($f$) to 2 cpp, θ to -0.441 radians, and kept the linear coefficients–α and β–as free parameters, which were fitted to the psychophysical data using an adaptive Bayesian algorithm [21].

Overall, the fitted psychometric curves match the empirical data with a high goodness of fit (median r-squared=0.9321). Such an agreement between psychometric curves and empirical data achieved with the frequency parameter constrained by the Fourier analyses further indicates a reliable frequency doubling effect in all our participants.

**Discussion.** The results of Experiment 2 clearly demonstrate the existence of a frequency-doubling effect in the perceived simultaneity of periodic audiovisual stimuli. Given that the frequency doubling effect is only expected to occur if audiovisual synchrony is computed over unsigned transient input channels, the present results support a dominance of transient input channels in multisensory time perception. These results complement the conclusions of Experiment 1 and together demonstrate the key role of transient input channels in audiovisual integration.

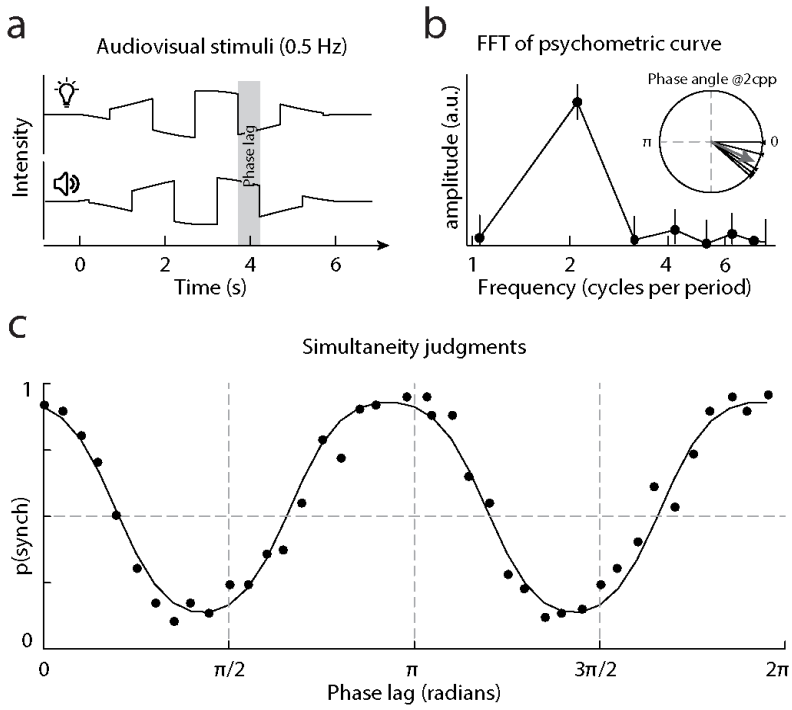


***Figure 3. Experiment 2, stimuli and results**. **A.** Schematic representation of the periodic stimuli. **B.** Frequency domain representation of the psychometric function: note the amplitude peak at 2 cycles per period. Errorbars represent the 99% confidence intervals. The inset represents the phase angle of the 2 cycles per period frequency component for each participant (thin lines), and the average phase (arrow). **C.** Results of Experiment 2 and psychometric fit, averaged across all participants. Each dot corresponds to 75 trials.*

**Modelling**

To account for multisensory integration, we have previously proposed a computational model, the Multisensory Correlation Detector (MCD, [18]), that exploits the temporal correlation between the senses to solve the correspondence problem, detect simultaneity and lag across the senses, and perform Bayesian-optimal multisensory integration. Based on the Hassenstein-Reichardt motion detector [22], the core of the MCD is composed of two mirror-symmetric subunits, each multiplying visual and auditory input after applying a low-pass filter to each of them. As a consequence of this asymmetric filtering, each subunit is selectively tuned to different temporal order of the signals (that is, vision vs. audition lead). The outputs of the two subunits are then combined in different ways to detect the correlation and lag of multisensory signals, respectively. Specifically, correlation is calculated by multiplying the outputs of the subunits, hence producing an output ($MCD_{Corr}$) whose magnitude represents the correlation between the signals (Figure 4C). Temporal lag is instead detected by subtracting the outputs of the subunits, like in the classic Hassenstein–Reichardt detector [22]. This yields an output ($MCD_{Lag}$) with a sign that represents the temporal order of

the signals (Fig. 4B). While a single MCD unit can only perform temporal integration of multisensory input, a population of MCD units, each receiving input from spatially-tuned receptive fields (Figure 4D), followed by divisive normalization (Figure 4E, see [23]), can perform Bayesian-optimal spatial cue integration (e.g., see [24]) for audiovisual source localization (Figure 4F, see [18] for details).

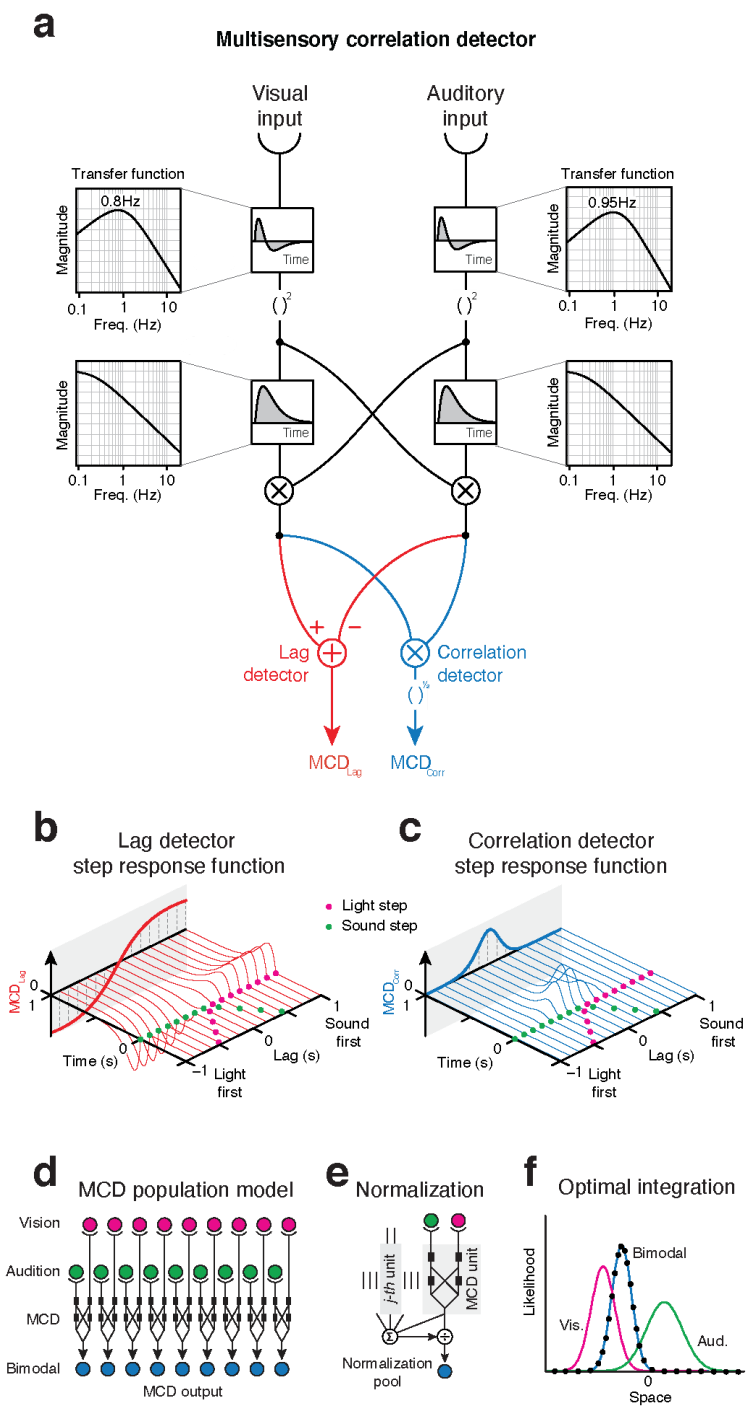


***Figure 4. MCD model.*** *A. Model schematics: the impulse-response functions of the channels are represented in the small boxes, and call-outs represent the transfer functions.* ***B.*** *Lag detector step responses as a function of the lag between visual and acoustic steps.* ***C.*** *Correlation detector responses as a function of the lag between visual and acoustic steps.* ***D.*** *Population of MCD units, each receiving input from spatiotopic receptive fields.* ***E.*** *Normalization, where the output of each unit is divided by the sum of the activity of all units.* ***F.*** Optimal integration of audiovisual spatial cues, as achieved using a population of MCDs with divisive normalization. Lines represent the likelihood functions for the unimodal and bimodal stimuli; dots represent the response of the MCD model, which is indistinguishable from the bimodal likelihood function.

In its original form, the input to the MCD consisted of sustained unimodal channels, modelled as low-pass temporal filters (see also, [20,25]. Although such a model could successfully account for the integration of trains of audiovisual impulses, the MCD cannot replicate the present results: for that, we first need to feed the model with unsigned transient unimodal input channels. Therefore, we replaced the front-end low-pass filters with band-pass temporal filters (to detect transients) followed by a squaring non-linearity (to get the unsigned transient [7]), and tested the model against the results of both Experiments (1 and 2), plus a variety of previously published psychophysical studies.

The equations of the revised MCD model are reported in the Supplementary Information. Just like the original version, the revised MCD model has three free parameters, representing the time constants of the two band-pass filters (one per modality) and that of the low-pass temporal filters of the subunits of the detector. Given that the tuning of the time constants of the model depends on the temporal profile of the input stimuli (see [26], here we used the data from Experiments 1 and 2 to constrain the temporal constants for the simulation of datasets consisting of either step stimuli or variations thereof (e.g., periodic stimuli), while for the simulation of experiments relying on stimuli with faster temporal rates, we constrained the temporal constants using data from Parise and Ernst [18]. Details on parameter fitting are reported in the methods section. Given that in a previous study [18] we have already shown that alternative models for audiovisual integration are not flexible enough to reproduce the wide gamut of psychophysical data successfully accounted for by our model, here we only consider the MCD model (in its revised form). A Matlab script with the full implementation of the revised MCD model will be made publicly available before publication.

**Simulation of Experiments 1 and 2.** To test whether an MCD that receives input from unimodal transient channels could replicate the results of Experiments 1 and 2, we fed the stimuli to the detector and used the $\overline{MCD_{Corr}}$ (Equation 8) output to model simultaneity judgments, and the $\overline{MCD_{Lag}}$ (Equation 9) for the temporal order judgments (see [18]). Given that the psychophysical data consisted of response probabilities (i.e., probability of "synchronous" responses for the SJ and probability of "audio first" responses in the TOJ), whereas the outputs of the model are continuous variables expressed in arbitrary units, we used a GLM with a probit link function to transform the output of the MCD into probabilities (Figure 5A, see also [18], for a detailed description of the approach). The linear coefficients

(i.e., slope and intercept) were fitted separately for each condition and task so that each psychometric curve had two free parameters for the GLM. The three parameters defining the temporal constants of the MCD model, instead, were fitted using all data from Experiments 1 and 2 combined using an adaptive Bayesian algorithm [21].

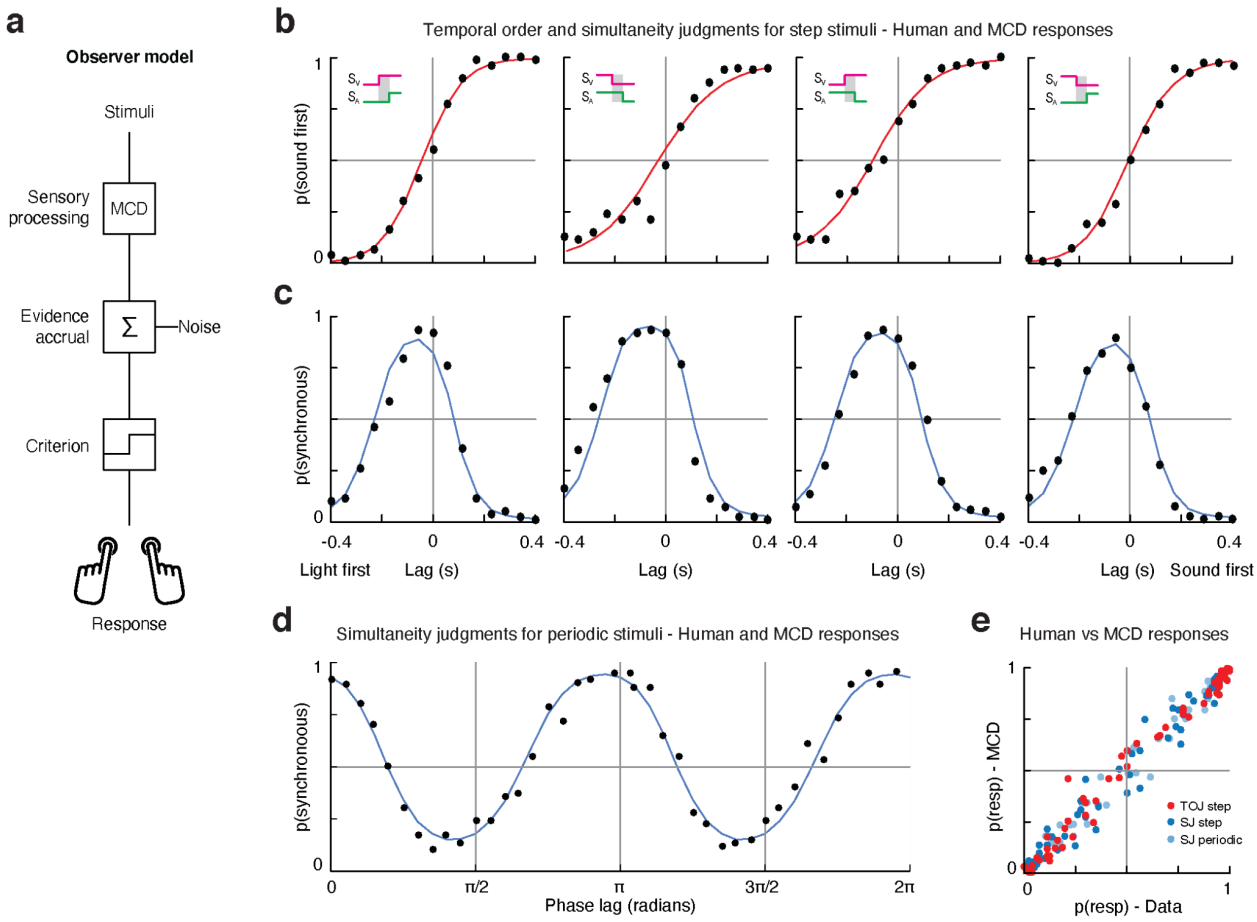


***Figure 5. MCD simulations of Experiments 1 and 2**. **A.** Schematics of the observer model, which receives input from one MCD unit to generate a behavioural response. The output of the MCD unit is integrated over a given temporal window (whose width depends on the duration of the stimuli), and corrupted by late additive noise before being compared to an internal criterion to generate a binary response. Such a perceptual decision-making process is modelled using a generalised linear model (GLM), depending on the task, the predictors of the GLM were either* $\overline{MCD}_{Corr}$ *(Equation 8) or* $\overline{MCD}_{Lag}$ *(Equation 9). **B** . Responses for the TOJ task of Experiment 1 (dots) and model responses (red curves). **C.** Responses for the SJ task of Experiment 1 (dots) and model responses (blue curves). **D.** Experiment 2 human (dots) and model responses (blue curve). **E.** Scatterplot of human vs model responses for both experiments.*

Overall, the model could tightly replicate the results of our experiments (Figure 5B-D): the Pearson correlation between the psychophysical data and model responses, computed across all conditions and participants was 0.99 for the SJ task of Experiment 1, 0.99 for the TOJ task of Experiment 1, and 0.97 for Experiment 2 (Figure 5E, see Supplementary Table 1). For comparison, the correlation between the data and the psychometric fits for Experiment 1 (i.e., cumulative Gaussians for the TOJs and difference of two cumulative Gaussians for the SJ) was 0.97, and 0.98 for Experiment 2; however, the psychometric fits required nearly twice as many free parameters compared to the model fits, and do not account for the generative process that give rise to the observed data. Importantly, just like human responses, the responses of the revised MCD model were nearly identical across all conditions in Experiment 1, whereas in Experiment 2 they displayed a clear frequency doubling effect. Furthermore, unlike the psychometric fits, which require to specify a priori the shape of the fitting function (e.g., sigmoid, bell, or periodic), the MCD model provides an output without specifying a priori any shape for the psychometric function. As shown in Figure 5B-D the model naturally captures the shape of the psychometric data. For instance, the same MCDcorr output could generate bell-shaped response distributions in Experiment 1 and sinusoidal responses in Experiment 2, purely based on the features of the input signals (such as its periodicity, or lack thereof). Therefore, taken together, the present simulations demonstrate that multisensory perception does indeed operate on correlated input from unimodal transient channels.

**Validation of the MCD through simulation of published results**

Although the simulations of Experiments 1 and 2 demonstrate that an MCD unit that receives input from transient unimodal channels is capable of reproducing the present psychophysical results, it is important to assess the generalizability of this approach. Therefore, we relied on the previous literature on multisensory perception of correlation, simultaneity and lag, as well as on the performance on crossmodal detection tasks, to validate our computational framework, and to assess its generalizability (by comparing the MCD responses against human performance on tasks not originally designed around our model). To this end, we selected a series of studies that employed parametric manipulations of the temporal structure of the signals, we simulated the stimuli, and we used the MCD model to predict human performance. If an MCD unit that receives input from transient unimodal channels is indeed the elementary computational unit for multisensory temporal processing,

we should be able to reproduce all of the earlier findings on multisensory perception with this revised MCD model. A summary of our simulations, listing the sample size, the number of observers, and the Pearson correlation of MCD and human responses, is reported in Table S1.

**Causality and temporal order judgments for random sequences of audiovisual impulses.** When we first proposed the MCD model [18], we tested it against a psychophysical experiment in which participants were presented with a random sequence of 5 clicks and 5 flashes over an interval of 1 second (Supplementary Figure S3A), and had to report whether the signals appeared to share a common cause (causality judgments) and which modality came first (temporal order judgment). To test whether the revised MCD model could also account for these previous findings, we fed the same stimuli to the model, and used the $\overline{MCD_{Corr}}$ (Eq. 8) output to simulate causality judgments, and $\overline{MCD_{Lag}}$ (Eq. 9) to simulate temporal order judgments. Given that the stimuli in this experiment had a much higher temporal rate than the stimuli used in Experiments 1 and 2, the temporal constants of the MCD were set as free parameters that we fitted to the experimental data. Due to the stochastic nature of the stimuli, we analysed the data using reverse correlation (Supplementary Figure S3B). The temporal constants of the MCD were fitted to maximize the Pearson correlation between the empirical and simulated responses, for both causality and temporal order judgments (for details on modeling and reverse correlation analyses, see Supplementary Figure S3B and [18]).

Overall, the model faithfully reproduced the experimental data, and the Pearson correlation between empirical and simulated classification images was 0.99 (Figure 6A-B). This result closely replicates the original simulations [18] performed with a version of the MCD that instead received input from sustained unimodal temporal channels (not transient as the current model). Given the differences between transient and sustained temporal channels, it may seem surprising that the two models are in such close agreement in the current simulation. However, it is important to remember that the stimuli in these experiments consisted of impulses (clicks and flashes), and the impulse response function of the sustained and transient channels as modeled in this study are indeed very similar. Therefore, such an agreement between the responses of the original and the revised versions of the MCD are indeed expected. Beside proving that the revised model can replicate previous results, this

simulation allowed us to estimate the temporal constants of the MCD for trains of clicks and flashes, which was necessary for the next simulations.

**Causality judgments for random sequences of audiovisual impulses with high temporal rates.** To identify the temporal features of the stimuli that promote audiovisual integration, Locke and Landy ([27], Experiment 2) ran a psychophysical experiment that was very similar to the causality judgment task described in the previous section. Although the stimuli in the two studies were nearly identical, the temporal sequences used by Locke and Landy [27] had a considerably higher temporal rate (range 8-14 impulses/s), longer duration (2s) and a more controlled temporal structure (Supplementary Figure S4). Participants observed the stimuli and performed a causality judgment task, whose results demonstrated that the perception of a common cause depended both on the correlation in the temporal structure of auditory and visual sequences (Figure 5C, left) and the maximum lag between individual clicks and flashes (Figure 5C, right).

Given the similarity of this study with the causality judgment of Parise and Ernst (2016), we followed the same logic described above to perform reverse correlation analyses (without smoothing the cross-correlograms). Moreover, the MCD simulations were performed with the same temporal constants used for the simulations of Parise and Ernst [18], so that this experiment is simulated with a fully-constrained model, with zero free parameters. Unlike our previous experiment, however, the stimuli used by Locke and Landy [27] varied in temporal rate, and hence also the number of clicks and flashes differed across trials. Given that the MCD is sensitive to the total stimulus energy, we normalized the model responses by dividing the $\overline{MCD_{Corr}}$ (Eq. 8) output by the rate of the stimuli.

Reverse correlation analyses were performed at the single subject level using both participants and model responses (see [18], for details on how the continuous model output of the MCD was discretized into a dichotomous variable), and the average data is shown in Figure 6C (left panel). Overall, the MCD model could near-perfectly predict the empirical classification image (Pearson correlation>0.99). Besides the reverse correlation analyses, Locke and Landy (2017) measured how the maximum lag between individual clicks and flashes affected the perceived common cause of audiovisual sequences. The results, shown in Figure 6C (right panel), demonstrate that perception of a common cause decreased with

increasing maximum audiovisual lag. Once again, the MCD model accurately predicts this finding (Pearson correlation=0.98) without any free parameters. Taken together, the present simulations demonstrate that the MCD model can account for the perception of a common cause between stochastic audiovisual sequences, even when the stimuli have a high temporal rate, and highlight the importance of both similarity in the temporal structure and crossmodal lag in audiovisual integration.

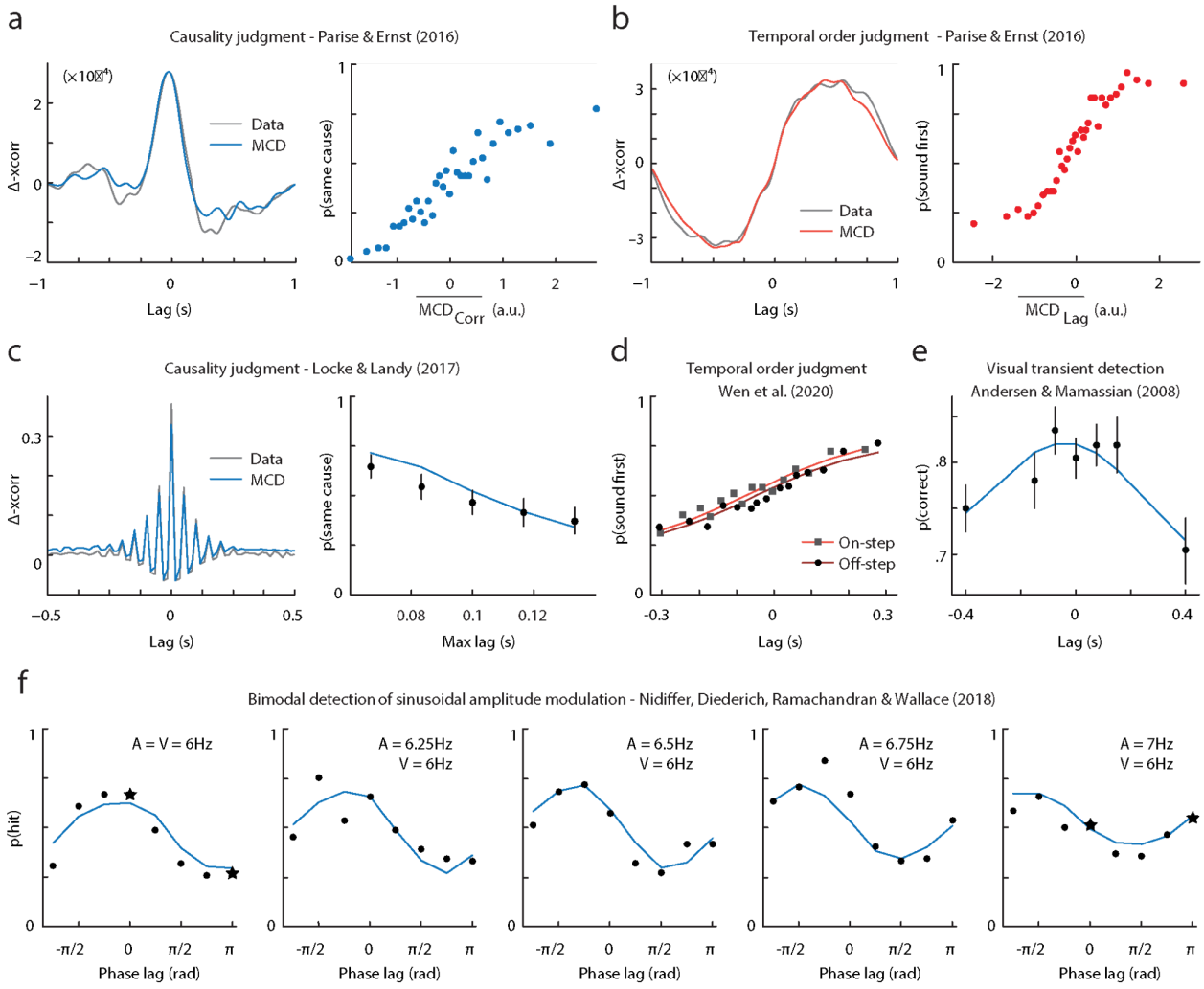


***Figure 5. MCD simulations of published results***. ***A***. *Results of the causality judgment task of Parise & Ernst (2016). The left panel represents the empirical classification image (grey) and the one obtained using the MCD model (blue). The right panel represents the output of the model plotted against human responses. Each dot corresponds to 315 responses.* ***B***. *Results of the temporal order judgment task of Parise & Ernst (2016). The left panel represents the empirical classification image (grey) and the one obtained using the MCD model (red). The right panel represents the output of the model plotted against human responses. Each dot corresponds to 315 responses.* ***C***. *Results of the causality judgment task of Locke & Landy (2017). The left panel represents the empirical classification image (grey) and the one obtained using the MCD model (blue). The right panel represents the effect of maximum audiovisual lag on perceived causality. Each dot represents on average 876*

*trials (range=[540, 1103]).* ***D****. Results of the temporal order judgment task of Wen et al. (2020). Squares represent the onset condition, whereas circles represent the offset condition. Each dot represents ≈745 trials.* ***E.*** *Results of the detection task of Andersen and Mamassian (2008), showing auditory facilitation of visual detection task. Each dot corresponds to 336 responses.* ***F.*** *Results of the audiovisual amplitude modulation detection task of Nidiffer and colleagues (2018), where the audiovisual correlation was manipulated by varying the frequency and phase of the modulation signals. Each dot represents ≈140 trials. The datapoint represented by a star correspond to the stimuli displayed in Supplementary Figure S7.*

**Temporal order judgment for onset and offset stimuli.** To investigate the perceived timing of auditory and visual on- and offsets, Wen and colleagues [28], presented continuous audiovisual noise stimuli with step on- and offsets (Supplementary Figure S5). The authors parametrically manipulated the audiovisual lag between either of the onset or the offset of the audiovisual stimulus and asked participants to report the perceived temporal order of the corresponding on- or offset, respectively. Despite large variability across participants, the point of subjective simultaneity systematically differed across conditions, with acoustic stimuli more likely appearing to change before the visual stimuli in the onset as compared to the offset condition.

To test whether the model could replicate this finding, we generated audiovisual signals with the same temporal manipulations of audiovisual lag and fed them to the MCD. To minimize the number of free parameters, we ran the simulation using the temporal constants of the filters fitted using the data from Experiments 1 and 2 (see above). Moreover, to test whether the MCD alone could predict the PSS shift between the onset and offset condition, we combined the data from all participants, and used a single GLM to link $\overline{MCD_{Lag}}$ (Eq. 9) to the TOJ data, irrespective of condition. Therefore, this simulation consisted of just two free parameters (i.e., the slope and intercept of the GLM). Overall, the responses of the MCD were in excellent agreement with the empirical data (Pearson correlation=0.97) and successfully captured the difference across onset and offset condition (Figure 6D). For comparison, the Pearson correlation between the data and the psychometric functions (modeled as cumulative Gaussians, fitted independently for onset and offset conditions) was also 0.97, but required twice as many free parameters (two per condition), and it does not account for the underlying sensory information processing.

**Acoustic facilitation of visual transients' detection.** To study the temporal dynamic of audiovisual integration of unimodal transients, Andersen and Mamassian ([14], Experiment 2) asked participants to detect a visual transient (i.e., a luminance increment) presented slightly

before or after a task-irrelevant acoustic transient (i.e., a sound intensity increment, Supplementary Figure S5). The task consisted of a two-interval forced-choice, with the visual stimuli set at 75% detection threshold, and the asynchrony between visual and acoustic transients parametrically manipulated using the method of constant stimuli.

To simulate this experiment, we fed the stimuli to the MCD model, and used a GLM to link the $\overline{MCD_{Corr}}$ (Eq. 8) responses to the proportion of correct responses. The temporal constants of the model were constrained based on the results of Experiments 1 and 2, so that this simulation had two free parameters: the slope and the intercept of the GLM. Overall, the MCD could reproduce the data of Andersen and Mamassian [14], and the Pearson correlation between data and model responses was 0.91 (Figure 6E).

**Detection of sinusoidal amplitude modulation.** To test whether audiovisual amplitude modulation detection depends on the correlation between the senses, Nidiffer and colleagues ([29], Experiment 2) asked participants to detect audiovisual amplitude modulation. Stimuli consisted of a pedestal intensity to which (in some trials) the authors added a near-threshold sinusoidal amplitude modulation (Supplementary Figure S6A). To manipulate audiovisual correlation, the authors varied the frequency and phase of the sinusoidal modulation signal. Specifically, the frequency of auditory amplitude modulation varied between 6Hz and 7Hz (5 steps), while the phase shift varied between 0 and 360 deg (8 steps). The frequency and phase shift of visual amplitude modulation were instead constant and set to 6Hz and 0 deg, respectively.

Both phase and frequency systematically affected participants' sensitivity; however, the results do not show any evidence of a frequency-doubling effect. This is a surprising finding: given the analogy between this study and our Experiment 2, a frequency doubling effect should be intuitively expected (if, as we claim, correlation detection relied on transient input channels). Indeed, when the amplitude modulations in the two modalities are 180 deg out of phase, the modulation signals are negatively correlated, and negatively correlated signals become positively correlated once fed to unsigned transient channels (Supplementary Figure S6A, bottom-left stimuli). When calculating the Pearson correlation of pairs of audiovisual signals, however, we should consider the whole stimuli, not just their amplitude modulations. Indeed, the stimuli used by Nidiffer and colleagues (2018) also consisted of linear ramps at onset and offset and a pedestal, compared with which the depth of the amplitude modulation

was barely noticeable (i.e., the modulation depth was about 6% of the pedestal level). Therefore, once the audiovisual correlation is computed while also considering the ramps (see scatterplots in Supplementary Figure S6A), the lack of a frequency doubling effect becomes apparent: all stimuli used by Nidiffer and colleagues (2019) are strongly positively correlated, though such a correlation slightly varied across conditions (being 1 when amplitude modulation had the same frequency in both modalities and zero phase shift, and 0.8 in the least correlated condition, see Supplementary Figure S6A-B).

To simulate the experiment of Nidiffer and colleagues [29], we fed the stimuli to the model and used the $\overline{MCD_{Corr}}$ (Eq. 8) output and a GLM to obtain the hit rate for the detection task. Given that neither the temporal constants of the MCD optimized for the Experiment 1 and 2, nor those optimized for Parise and Ernst [18], provided a good fit for Nidiffer's data, we set both the temporal constants of the MCD and the slope and intercept of the GLM as free parameters. All-in-all, the model could replicate the results of Nidiffer and colleagues [29], and the Pearson correlation between the model and human responses was 0.89.

## CONCLUSIONS

Taken together, the present results demonstrate the dominance of transient over sustained channels in audiovisual integration. Based on the assumption that perceived synchrony across the senses depends on the (Pearson) correlation of the unimodal signals [17], we generated specific hypotheses for perceived audiovisual synchrony - depending on whether such a correlation is computed over transient or sustained inputs. Such hypotheses were then tested against the results of two novel psychophysical experiments, jointly showing that Pearson correlation between transient input signals systematically determines the perceived timing of audiovisual events. Based on that, we revised a general model for audiovisual integration, the Multisensory Correlation Detector (MCD), to selectively receive input from unimodal transient instead of sustained channels. Inspired by the motion detectors originally proposed for insect vision, such a biologically-plausible model integrates audiovisual signals through correlation detection, and could successfully account for the results of our psychophysical experiments along with a variety of recent findings in multisensory research. Specifically, once fed with transient input channels, the model could replicate human temporal order judgments, simultaneity judgments, causality judgments and crossmodal signal detection

under a broad manipulation of input signals (i.e., step stimuli, trains of impulses, sinusoidal envelopes, etc.).

Previous research has already proposed a dominance of transient over sustained channels in audiovisual perception, with evidence coming from both psychophysical detection tasks and neuroimaging studies [14,15]. However, the role of transient and sustained channels on the perceived timing of audiovisual events (arguably the primary determinant of multisensory integration) has never been previously addressed, let alone computationally framed within a general model of multisensory integration. This study fills this obvious gap and explains all such previous findings in terms of the response dynamics of the MCD model, thereby demonstrating that audiovisual integration relies on correlated input from unimodal transient channels. Recent research, however, criticized the MCD model for its alleged inability to either process audiovisual stimuli with a high temporal rate or detect signal correlation for short temporal intervals [27,30]. By receiving inputs from transient unimodal channels, this revised version of the model fully addresses such criticisms. Indeed, the new MCD can near perfectly predict human performance in a causality judgment task with stimuli with a high temporal rate (up to 18Hz) using the same set of parameters optimized for stimuli with a much lower rate (5Hz), with a Pearson correlation coefficient of 0.99.

While MCD simulations could replicate the shape of the empirical psychometric curves, standard psychometric functions can also fit the same datasets, sometimes with even higher goodness of fit. Hence one might wonder what the advantage of the current modelling approach is. However, when comparing MCD simulations with psychometric fits, it is important to focus on the differences between these two modelling approaches. Psychometric functions usually relate some physical parameter (the independent variable) to a measure of performance (the dependent variable)-based on statistical considerations regarding the stimuli and the underlying perceptual decision-making process. For example, based on assumptions on the nature of the bell-shaped distribution of audiovisual simultaneity judgments, Yarrow and colleagues proposed a model for simultaneity judgments that fits the SJ data of our Experiment 1 just as well as the MCD model (though with a larger number of free parameters). Psychometric curves for SJs, however, are not always bell-shaped: for example, in Experiment 2, they are sinusoidal. This finding is naturally captured by the MCD model but not by models that enforce some specific shape for the psychometric functions. The reason is that statistical approaches to psychometric curve fitting are usually agnostic as to

how the raw input signals are transformed into evidence for perceptual decision-making. Indeed, while the inputs for psychometric fits are some parameters of the stimuli (e.g., the amount of audiovisual lag), the inputs for the MCD simulations are the actual stimuli themselves. That is the MCD extracts from the raw signals the evidence that is then fed into the perceptual decision-making process (i.e., the observer model, Figure 5A). By making explicit all the processing steps that link the input stimuli to a button press, the MCD model can tailor its predictions to any input stimuli, with the shape of the psychometric curves being unconstrained in principle, yet fully predictable based only on the input signals and the experimental task. This is why the same MCD model can predict bell-shaped psychometric functions in the SJ task of Experiment 1, sigmoidal functions in the TOJ task of Experiment 1, and sinusoidal functions in Experiment 2; whereas three different functions were necessary for the psychometric fits of the same experiments. Moreover, unlike psychometric fits, the MCD model is a biologically inspired neural model ; as such it not only allows one to account for behavioural responses, but also for neurophysiological data, as recently shown through magnetoencephalography [26].

Previous research attributed the multisensory benefits on perceptual decision-making tasks to “late”, post-sensory changes occurring at the level of the decision dynamics-with evidence stemming from EEG activity in brain regions commonly considered to be involved in “high-level”, decision-making [31]. While the present study cannot directly address such neurophysiological considerations, the computational framework proposed here, however, challenges any post-sensory interpretations. Indeed, the model proposed in this study can be divided into two separate components: the MCD, which handles the “early” sensory processing stage, and a “late” observer model, which receives input from the MCD and uses this information (along with the task demands) to generate a perceptual classification response (i.e., a button-press). In this context, it is important to note how multisensory benefits in detection tasks critically depend on the correlation and timing of audiovisual events: namely, the two factors that mostly affect the responses of the MCD model (e.g., see Figure 5E-F). Therefore, it is not surprising to see that the current framework can account for the effects of stimulus timing on performance purely based on the dynamics of the MCD responses, with no need for ad-hoc adjustments in the perceptual decision-making process. Further studies will hopefully reconcile such discrepant interpretations on the origins of multisensory benefits on perceptual decision-making tasks, possibly through a better understanding of the

computations underlying the electrophysiological correlates recorded with modern imaging techniques.

Although the present study unequivocally supports a dominance of transient channels in multisensory integration, it is still necessary to consider which role, if any, sustained channels may play in crossmodal perception. Indeed, earlier studies have shown that sustained information, such as the intensity of visual and acoustic stimuli does indeed systematically affect performance in behavioural tasks [32,33], and can even elicit phenomena known as crossmodal correspondences [34]. The mapping of intensity between vision and audition, however, is a somewhat peculiar one, as it is not obvious whether increasing intensity in one modality is mapped to higher or lower intensity in the other (that is, an obvious mapping between acoustic and lightness intensity, rooted in natural scene statistics, has not been reported, yet). A perhaps more profound mapping between sustained audiovisual information relates to redundant cues, that is, properties or a physical stimulus that can be jointly estimated via two or more senses; such as the size of an object, which can be simultaneously estimated through vision and touch [35]. This is a particularly prominent aspect of multisensory perception, and the estimated size of an object is arguably sustained, rather than transient stimulus information. While the present study cannot directly address such a question, we propose that the correlation between visual and tactile transients, like those occurring when we reach and make contact with an object, is what the brain needs to solve the correspondence problem; and that hence let us infer that what we see and touch are indeed coming from the same distal stimulus. Then, once made sure that the spatial cues that we get from vision and touch are redundant, size information can be optimally integrated. Testing such a hypothesis is surely a fertile subject for future research.

Finally, it is important to consider what are the advantages of transient over sustained stimulus information for multisensory perception. An obvious one is parsimony, as dropping information that does not change over time entails lower transmission bandwidth by minimizing redundancy through efficient input coding (Barlow, 1961). Therefore, by only representing input variations, transient channels operate as event detectors, signalling the system of potentially relevant changes in the surrounding. Interestingly, a similar approach has grown in popularity in novel technological applications, such as neuromorphic circuits and event cameras. Indeed, while traditional sensors operate on a frame-based approach, whereby inputs are periodically sampled based on an internal clock, event cameras only

respond to external changes in brightness as they occur, thereby reducing transmission bandwidth and maximizing dynamic range. Interestingly, recent work has even successfully exploited Hassenstein-Reichardt detectors as a biologically inspired solution for detecting motion with event cameras [36]. Hence, considering the mathematical equivalence of the MCD and the Hassenstein-Reichardt detectors, the present study suggests the intriguing possibility of using the revised MCD model as a biologically inspired solution for sensory fusion in future multimodal neuromorphic systems.

# Supplementary information

## The MCD model

The modified MCD model closely resembles the original model, but it takes input from unimodal transient (instead of sustained) input channels. That is, rather than being simply low-pass filtered, time-varying visual and auditory signals ($S_V(t)$, $S_A(t)$) are independently filtered by band-pass filters ($f$). Following Adelson and Bergen (1986), band-pass filters are modelled as biphasic impulse response functions defined as follows:

$$f_{mod}(t) = \frac{t}{\tau_{mod}} \cdot e^{\frac{-t}{\tau_{mod}}} \cdot \left(1 - \frac{t^2}{\tau_{mod}^2 \cdot n!}\right)$$

(Equation 1).

In this equation $\tau_{mod}$ is the modality-dependent temporal constant of the filter (mod=[a,v]). Based on the previous results of Experiments 1 and 2, we set these constants to be $\tau_V$=0.070 s and $\tau_A$=0.055 s for the visual and auditory filters, respectively. In line with Adelson and Bergen (1986), the parameter $n$ (which controls the negative lobe of the impulse response) is set to 3.

As in the original implementation of the MCD model, the low-pass temporal filter of the correlation unit was:

$$f_{av}(t) = \frac{t}{\tau_{av}} \cdot e^{\frac{-t}{\tau_{av}}}$$

(Equation 2)

The temporal constant $\tau_{av}$ was set to 0.674 s.

The filtered unisensory stimuli $Sf_{mod}(t)$ feeding into the correlation unit were obtained as follows:

$$Sf_{mod}(t) = [S_{mod}(t) * f_{mod}(t)]^2$$

(Equation 3)

where (*) represents the convolution operator. Filtered signals are squared before being summed to render the responses insensitive to the polarity of changes in intensity [7].

Like in the original MCD model, each sub-unit ($u_1$, $u_2$) of the detector independently combines filtered visual and auditory signals as follows:

$$u_1(t) = Sf_v(t) \cdot [Sf_a(t) * f_{av}(t)]$$ (Equation 4),

$$u_2(t) = Sf_a(t) \cdot [Sf_v(t) * f_{av}(t)]$$ (Equation 5).

To this end, the signals are convolved (*) with the low-pass temporal filters. The response of the sub-units is eventually multiplied or subtracted.

$$MCD_{corr}(t) = \sqrt{u_1(t) \cdot u_2(t)}$$ (Equation 6),

$$MCD_{corr}(t) = u_2(t) - u_1(t)$$ (Equation 7).

The resulting time-varying responses represent the local temporal correlation ($MCD_{Corr}$) and lag ($MCD_{Lag}$) across the signals. To reduce such time-varying responses into a single summary variable representing the total amount of evidence from each trial, we simply averaged the output of the detectors over a given temporal window of N samples:

$$\overline{MCD_{corr}} = \frac{1}{N}\sum_{t=1}^{N} MCD_{corr}(t)$$ (Equation 8),

$$\overline{MCD_{lag}} = \frac{1}{N}\sum_{t=1}^{N} MCD_{lag}(t)$$ (Equation 9).

In the present simulations, the width of the temporal window varies across experiments, due to the variable duration of the audiovisual stimuli. The output of the MCD model is eventually transformed into probabilities using a general linear model with a probit link function (assuming additive Gaussian noise; see Parise & Ernst, 2016, for a similar approach).

**Modelling sustained input channels**

In line with previous work [7,18,25], here we model sustained input channels as low-pass temporal filters with the following impulse response function:

$$f_{mod}(t) = \frac{t}{\tau_{mod}} \cdot e^{\frac{-t}{\tau_{mod}}}$$

(Equation 10).

where $\tau_{mod}$ is the modality-dependent temporal constant of the filter (mod=[a,v]). Such a low-pass filter has the same shape as the bimodal filters of the MCD (Equation 2) and of the unimodal filter of the original MCD model [18].

**Experiment 1: the relationship between the PSS and WSS measured using TOJs vs SJs**

TOJs and SJs are the two main psychophysical tasks to measure sensitivity to lags across the senses. With both tasks it is possible to estimate the point and window of subjective simultaneity; however, when measured on the same subjects, the point and window of subjective simultaneity measured from the two tasks are often not correlated [37–39]. This finding has been sometimes considered evidence for independent underlying neural mechanisms. Given that in Experiment 1, we estimated the PSS and WSS with both TOJs and SJs, we can repeat the same analyses on our dataset. Figure S1C shows the scatterplot of the PSS measured with the TOJ against the PSS measured with the SJ, and Figure S1D the scatterplot of the WSS measured with the TOJ against the SJ. Each point corresponds to one psychometric function in Supplementary Figure S1A. As in previous studies, the PSS and WSS measured with the two tasks are not significantly correlated (PSS: r=-0.16, p=0.38; WSS:r=0.16, p= 0.39).

While such a finding intuitively suggests the existence of independent mechanisms underlying the two tasks, our model clearly suggests otherwise. Indeed the MCD model provides two outputs: one representing the decision variable for the SJ (Equation 8), and the other for the TOJ (Equation 9). Therefore, we propose that TOJs and SJs share a common mechanism for sensory processing: the MCD model (Equations 1-7). However, the following decision-making processes (see Figure 5A) are independent across the two tasks, hence the lack of correlation between the PSS and WSS estimated using SJs vs TOJs.

**Sample size**

To properly substantiate our claims and quantitatively test our model, this study relies on a large collection of three novel psychophysical datasets, and six previously published ones. These consisted of behavioural responses from a variety of tasks such as temporal order judgments, simultaneity judgments, causality judgments and detection tasks, for a total of 68693 trials. Our Experiments 1 and 2 alone consisted of 12600 trials (4800 for the TOJ task in Experiment 1, 4800 for the SJ task in Experiment 1, and 3000 for Experiment 2). Given the nature of the present study, we were especially interested in determining the shapes of the psychometric functions, hence we prioritized collecting a large number of trials per observer (over a large pool of observers). Considering that we expected both large effect sizes (see Figure 1B-C) and low individual variability, the sample size of our new experiments is more than sufficient to draw reliable conclusions. Single subject analyses (Supplementary Figures S1 and S2), showing consistent behaviour across participants support our original assumptions.

Nevertheless, it is important to stress that our psychophysical experiments only represent a small fraction of the overall dataset used in this study to assess and model the contribution of transient and sustained channels in multisensory integration. Indeed, when calculating the sample size of this study, we must also include all the previously published datasets that were re-analyzed and simulated with the MCD model. Hence, our conclusions are supported by a large-scale analysis and computational modelling of a vast set of behavioural data, consisting of 68693 trials from a sample of 110 observers, collectively providing strong converging evidence for the dominance of transient over sustained input channels in multisensory integration (See Table).

The data from Experiments 1 and 2 will be made publicly available online once the paper is accepted for publication.

| Dataset | Task | Number of observers | Number of trials | N. trials for observer | MCD-data Correlation |
|---|---|---|---|---|---|
| Experiment 1 | Simultaneity judgment | 8 | 4800 | 600 | 0.99 |
| | Temporal order judgment | | 4800 | 600 | 0.99 |
| Experiment 2 | Simultaneity judgment | 5 | 3000 | 600 | 0.98 |
| Parise et al. (2016) | Causality judgment | 5 | 9300 | 1860 | 0.98 |
| | Temporal order judgment | | 9300 | 1860 | 0.99 |
| Locke et al. (2017) | Causality judgment | 10 | 7200 | 720 | 0.99 |
| Wen et al. (2020) | Temporal order judgment | 57 | 22337 | ≈392 | 0.97 |
| Andersen et al (2008) | Transient detection | 13 | 2352 | ≈181 | 0.91 |
| Nidiffer et al. (2018) | Modulation detection | 12 | 5604 | 467 | 0.89 |
| | **Overall** | **110** | **68693** | **≈624** | **0.97** |

***Table S1. Sample size of the datasets modelled and analysed in the present study.*** *Two of the datasets listed here (i.e., Experiment 1 and Parise et al., 2016) consisted of two tasks, each tested on the same pool of observers. The last row represents the total number of observers and trials, the average number of trials per participant, and the average correlation between MCD simulations and human data. Note how the revised MCD tightly replicated human responses in all of the datasets included in this study, despite major differences in stimuli, tasks, and sample sizes of the individual studies (see last column).*

| | $\chi^2$ | df | p-value |
|---|---|---|---|
| PSS (TOJ) | 6.15 | 3 | 0.1045 |
| PSS (SJ) | 2.85 | 3 | 0.4153 |
| WSS (TOJ) | 2.55 | 3 | 0.4663 |
| WSS (SJ) | 5.55 | 3 | 0.1357 |

***Table S2. Results of Friedman test for Experiment 1.*** *Four separate tests were used to assess whether the four experimental conditions differed in terms of PSS and WSS in the TOJ and SJ tasks. The first column represents the variables, the second the* $\chi^2$ *value, the third the degrees of freedom, and the fourth the p-value. Given that we ran four tests on the same dataset, statistical significance should be computed by comparing the p-value against a Bonferroni-adjusted alpha level of 0.0125 (i.e., 0.05/4).*

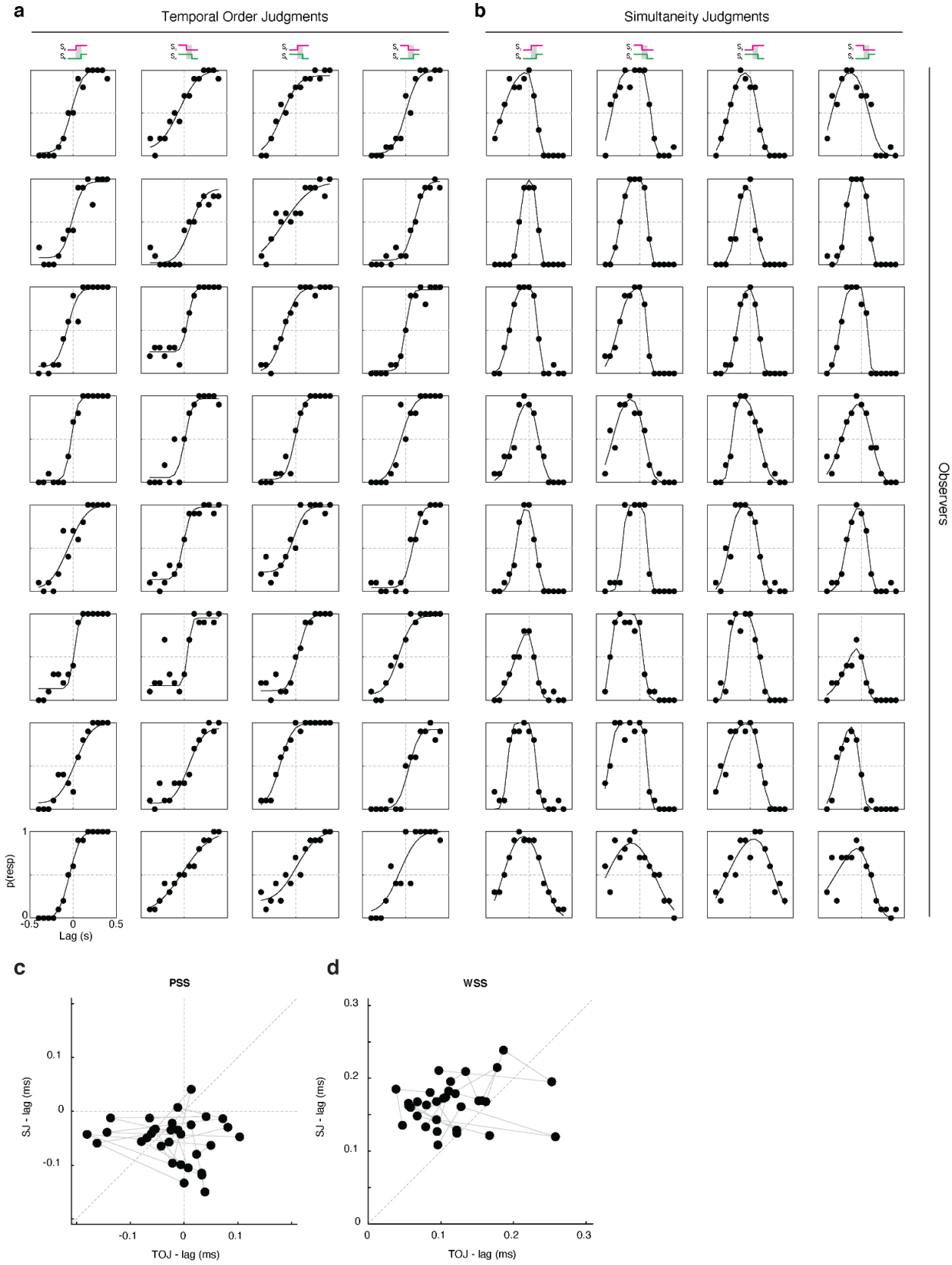
a
Temporal Order Judgments
b
Simultaneity Judgments
Observers
p(resp)
1
0
-0.5
0
0.5
Lag (s)
c
PSS
SJ - lag (ms)
0.1
0
-0.1
-0.1
0
0.1
TOJ - lag (ms)
d
WSS
SJ - lag (ms)
0.3
0.2
0.1
0
0
0.1
0.2
0.3
TOJ - lag (ms)

***Supplementary Figure S1. Results and psychometric fits of Experiment 1.*** *Data from different observers are represented in different rows.* ***A.*** *represent the data of the TOJ task,* ***B.*** *represent the data of the SJ task. The icons on top represent the different conditions. Each dot corresponds to 10 trials.* ***C.*** *represents the scatterplot of the PSS measured with the TOJ plotted against the PSS measured with the SJ.* ***D.*** *represents the scatterplot of the WSS measured with the TOJ plotted against the PSS measured with the SJ. Each dot in panels C and D represents the PSS or WSS from one condition and observer (that is, there are 4 dots for each observer, one per condition); datapoints from the same participant are linked by a grey line.*

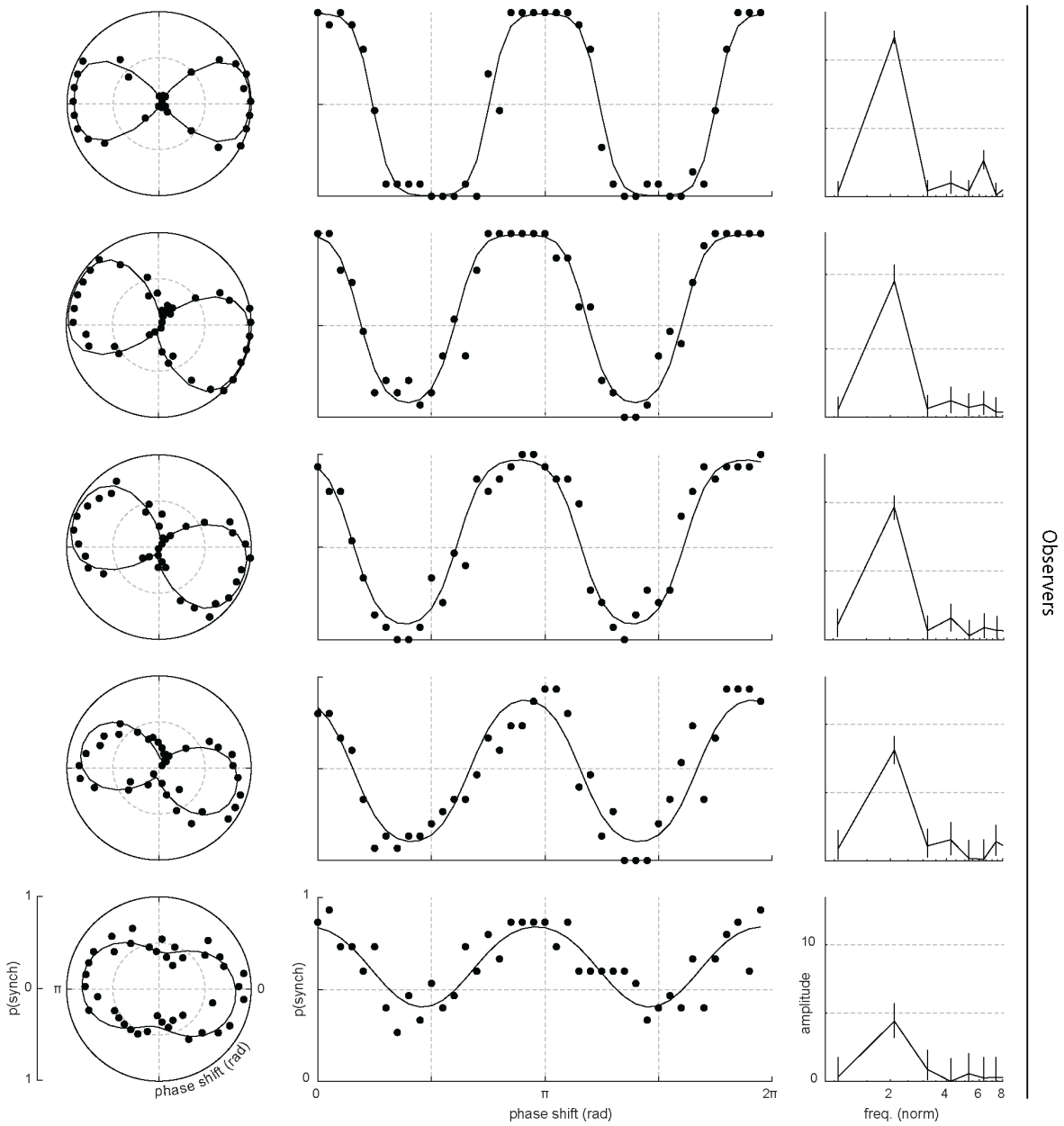


***Supplementary Figure S2. Results and psychometric fits of Experiment 2.*** *Data from different observers are represented in different rows. The first four column represent the data in polar coordinates, whereas the second column represent the same dataset in Cartesian coordinates. The counter-clockwise rotation of the polar psychometric functions indicate that maximum perceived synchrony across the senses occur when vision changes slightly before audition. Each dot corresponds to 15 trials. The last column represents the psychometric curve in the frequency domain: note the peak at 2cpp in every participant, indicating the frequency doubling effect. The errorbars in the last column represent the 99% confidence intervals.*

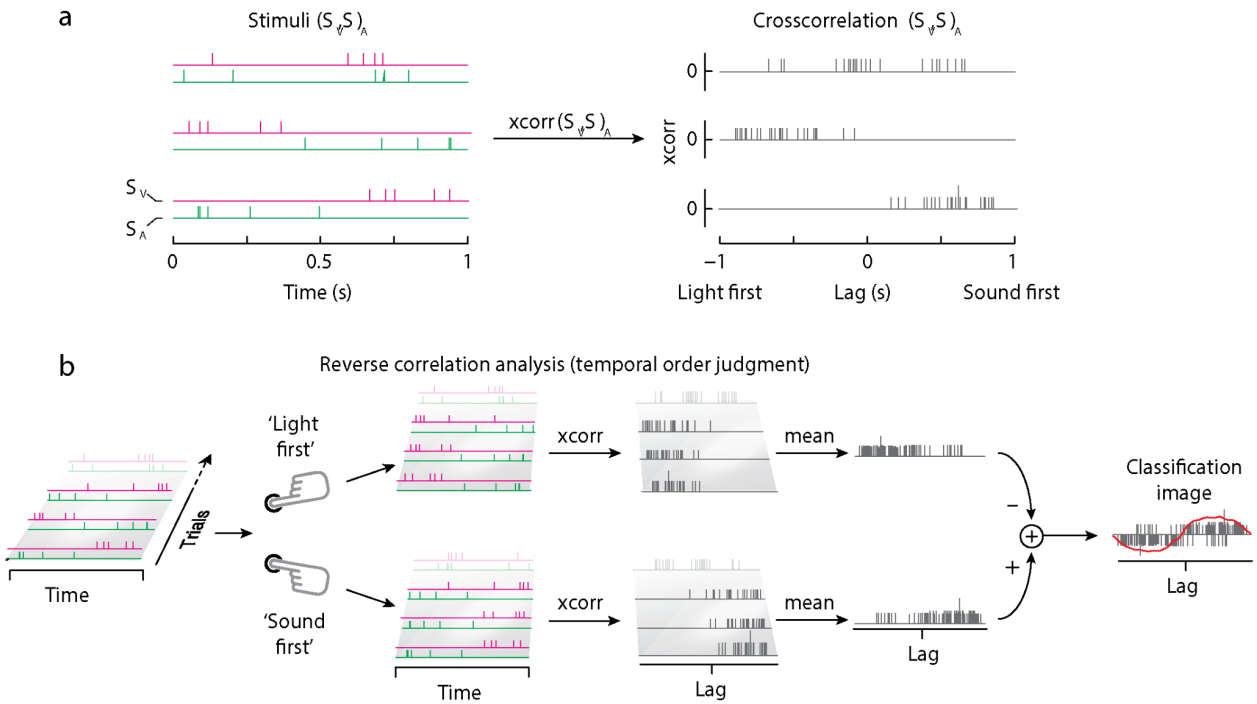


***Supplementary Figure S3. Stimuli and reverse correlation analyses of Parise & Ernst (2016).*** *Panel **A** represents three pairs of audiovisual stimuli (left), and their cross-correlation (right). Panel **B** shows a schematic representation of the reverse correlation analyses. This figure is adapted from [18].*

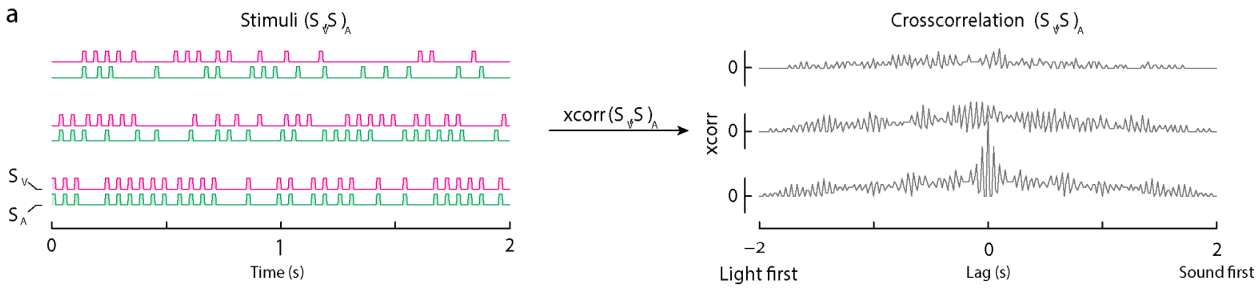


***Supplementary Figure S4. Stimuli of Locke & Landy (2017).*** *Three example pairs of audiovisual stimuli, and their cross-correlogram. Note how the stimuli vary in both terms of temporal rate (i.e., total number of clicks and flashes) and audiovisual correlation (with the bottom one being fully correlated).*

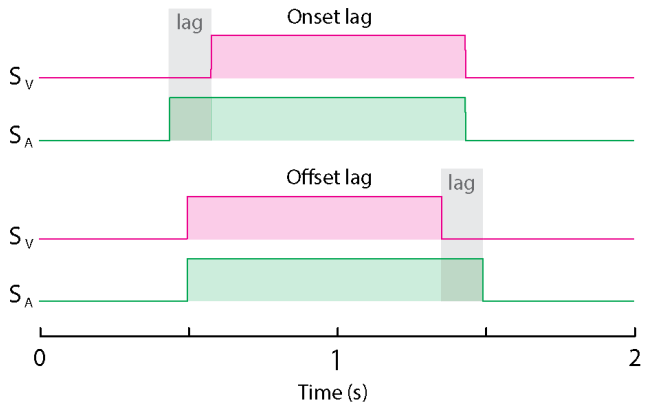


***Supplementary Figure S5. Stimuli of Wen et al. (2020).*** *Stimuli consisted of rectangular temporal envelopes, with a variable audiovisual lag either at the onset (top) or offset (bottom). The amount of audiovisual lag varied across trials, following a staircase procedure.*

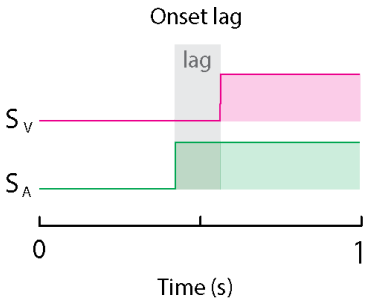


***Supplementary Figure S6. Stimuli of Andersen & Mamassian (2008).*** *Stimuli consisted of on-steps, with a parametrical manipulation of the lag between vision and audition, determined using the method of constant stimuli.*

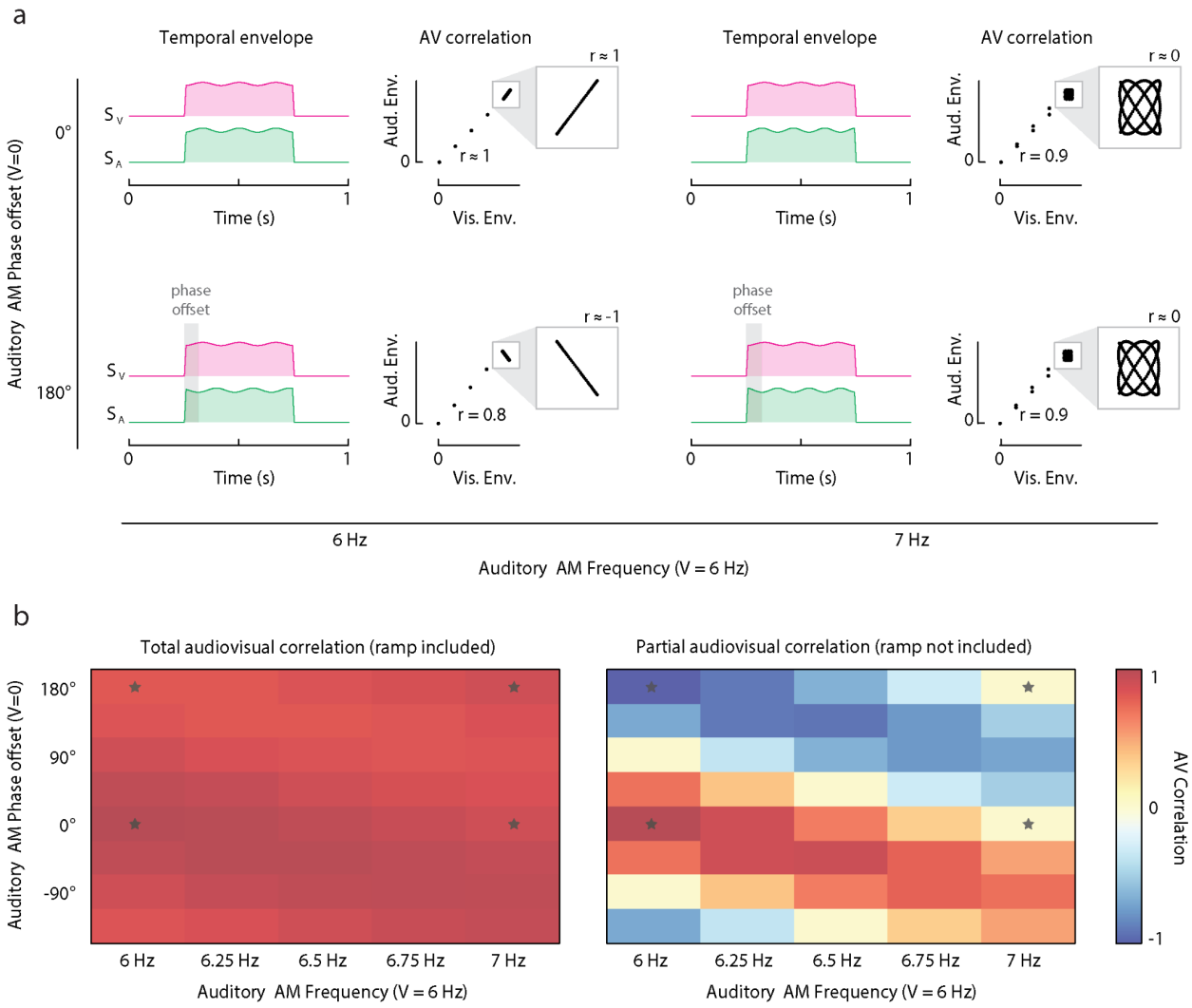


***Supplementary Figure S7. Stimuli of Nidiffer et al. (2018).*** *Stimuli consisted of a sinusoidal amplitude modulation over a pedestal intensity (Panel A). The pedestal had a 10ms linear ramp at onset and offset. While the visual sinusoidal amplitude modulation was constant throughout the experiment (frequency = 6Hz, zero phase offset), the auditory amplitude modulation varied in both frequency (from 6Hz to 7Hz, in 5 steps) and phase offset (from 0 to 360 deg, in 8 steps). Next to each pair of stimuli, we represent the scatterplot of the visual and auditory envelopes, which highlight the audiovisual correlation. The call-out boxes zoom in on the correlation between the audiovisual sinusoidal amplitude modulation (excluding the linear onset and offset ramps), whereas the main scatterplots also display the ramps. Panel B represents the audiovisual Pearson correlation for all the stimuli used by Nidiffer et al. The left panel shows the total audiovisual correlation, which was calculated while also including the onset and offset ramps; the right panel represents the partial correlation, calculated by only considering the sinusoidal amplitude modulation (i.e., the area inside the*

*call-outs in Panel A) without considering the onset and offset linear ramps (as done in Nidiffer et al., 2018). Note that once the ramps are included, all audiovisual stimuli are strongly correlated. The stars in the correlation matrices mark the cells corresponding to the four stimuli represented in Panel A, and the datapoints represented by a star in Figure 5F*

## References


1. Benucci A, Frazor RA, Carandini M. Standing waves and traveling waves distinguish two circuits in visual cortex. Neuron. 2007;55: 103–117.

2. Kim Y-J, Grabowecky M, Paller KA, Suzuki S. Differential roles of frequency-following and frequency-doubling visual responses revealed by evoked neural harmonics. J Cogn Neurosci. 2011;23: 1875–1886.

3. Breitmeyer BG, Ganz L. Implications of sustained and transient channels for theories of visual pattern masking, saccadic suppression, and information processing. Psychol Rev. 1976;83: 1–36.

4. Qin L, Chimoto S, Sakai M, Wang J, Sato Y. Comparison between offset and onset responses of primary auditory cortex ON-OFF neurons in awake cats. J Neurophysiol. 2007;97: 3421–3431.

5. Recanzone GH. Response profiles of auditory cortical neurons to tones and noise in behaving macaque monkeys. Hear Res. 2000;150: 104–118.

6. Ikeda H, Wright MJ. Receptive field organization of “sustained” and “transient” retinal ganglion cells which subserve different function roles. J Physiol. 1972;227: 769–800.

7. Stigliani A, Jeska B, Grill-Spector K. Encoding model of temporal processing in human visual cortex. Proc Natl Acad Sci U S A. 2017;114: E11047–E11056.

8. Stein BE. The New Handbook of Multisensory Processing. MIT Press; 2012.

9. Vroomen J, Keetels M. Perception of intersensory synchrony: a tutorial review. Atten Percept Psychophys. 2010;72: 871–884.

10. Sekuler R, Sekuler AB, Lau R. Sound alters visual motion perception. Nature. 1997. pp. 308–308. doi:10.1038/385308a0

11. van Wassenhove V, Grant KW, Poeppel D. Temporal window of integration in auditory-visual speech perception. Neuropsychologia. 2007;45: 598–607.

12. Samad M, Parise C, Keller S, Di Luca M. A common cause in the phenomenological and sensorimotor correlates of body ownership. Journal of Vision. 2018. p. 1230. doi:10.1167/18.10.1230

13. Parise CV, Spence C, Ernst MO. When correlation implies causation in multisensory integration. Curr Biol. 2012;22: 46–49.

14. Andersen TS, Mamassian P. Audiovisual integration of stimulus transients. Vision Res. 2008;48: 2537–2544.

15. Werner S, Noppeney U. The contributions of transient and sustained response codes to audiovisual integration. Cereb Cortex. 2011;21: 920–931.

16. Herdener M, Lehmann C, Esposito F, di Salle F, Federspiel A, Bach DR, et al. Brain responses to auditory and visual stimulus offset: shared representations of temporal edges. Hum Brain Mapp. 2009;30: 725–733.

17. Wei WWS. Time Series Analysis: Univariate and Multivariate Methods. Pearson College Division; 2006.

18. Parise CV, Ernst MO. Correlation detection as a general mechanism for multisensory integration. Nat Commun. 2016;7: 11543.

19. Parise CV, Spence C. “When birds of a feather flock together”: synesthetic correspondences modulate audiovisual integration in non-synesthetes. PLoS One. 2009;4: e5664.

20. Yarrow K, Jahn N, Durant S, Arnold DH. Shifts of criteria or neural timing? The assumptions underlying timing perception studies. Consciousness and Cognition. 2011. pp. 1518–1531. doi:10.1016/j.concog.2011.07.003

21. L Acerbi WJM. Practical Bayesian optimization for model fitting with Bayesian adaptive direct search. 2017. pp. 1–11.

22. Hassenstein B, Reichardt W. Systemtheoretische Analyse der Zeit-, Reihenfolgen- und Vorzeichenauswertung bei der Bewegungsperzeption des Rüsselkäfers Chlorophanus. Zeitschrift für Naturforschung B. 1956. pp. 513–524. doi:10.1515/znb-1956-9-1004

23. Ohshiro T, Angelaki DE, DeAngelis GC. A normalization model of multisensory integration. Nat Neurosci. 2011;14: 775–782.

24. Alais D, Burr D. The ventriloquist effect results from near-optimal bimodal integration. Curr Biol. 2004;14: 257–262.

25. Burr D, Silva O, Cicchini GM, Banks MS, Morrone MC. Temporal mechanisms of multimodal binding. Proceedings of the Royal Society B: Biological Sciences. 2009. pp. 1761–1769. doi:10.1098/rspb.2008.1899

26. Pesnot Lerousseau J, Parise CV, Ernst MO, van Wassenhove V. Multisensory correlation computations in the human brain identified by a time-resolved encoding model. Nat Commun. 2022;13: 2489.

27. Locke SM, Landy MS. Temporal causal inference with stochastic audiovisual sequences. PLOS ONE. 2017. p. e0183776. doi:10.1371/journal.pone.0183776

28. Wen P, Opoku-Baah C, Park M, Blake R. Judging Relative Onsets and Offsets of Audiovisual Events. Vision (Basel). 2020;4. doi:10.3390/vision4010017

29. Nidiffer AR, Diederich A, Ramachandran R, Wallace MT. Multisensory perception reflects individual differences in processing temporal correlations. Sci Rep. 2018;8: 14483.

30. Colonius H, Diederich A. Formal models and quantitative measures of multisensory integration: a selective overview. Eur J Neurosci. 2020;51: 1161–1178.

31. Franzen L, Delis I, De Sousa G, Kayser C, Philiastides MG. Auditory information enhances post-sensory visual evidence during rapid multisensory decision-making. Nat Commun. 2020;11: 5440.

32. Stein BE, London N, Wilkinson LK, Price DD. Enhancement of perceived visual intensity by auditory stimuli: a psychophysical analysis. J Cogn Neurosci. 1996;8: 497–506.

33. Odgaard EC, Arieh Y, Marks LE. Brighter noise: sensory enhancement of perceived loudness by concurrent visual stimulation. Cogn Affect Behav Neurosci. 2004;4: 127–132.

34. Parise C, Spence C. Audiovisual Cross-Modal Correspondences in the General Population.

Oxford Handbooks Online. 2013. doi:10.1093/oxfordhb/9780199603329.013.0039

35. Ernst MO, Banks MS. Humans integrate visual and haptic information in a statistically optimal fashion. Nature. 2002;415: 429–433.

36. D'Angelo G, Janotte E, Schoepe T, O'Keeffe J, Milde MB, Chicca E, et al. Event-Based Eccentric Motion Detection Exploiting Time Difference Encoding. Front Neurosci. 2020;14: 451.

37. García-Pérez MA, Alcalá-Quintana R. On the discrepant results in synchrony judgment and temporal-order judgment tasks: a quantitative model. Psychon Bull Rev. 2012;19: 820–846.

38. Linares D, Holcombe AO. Differences in perceptual latency estimated from judgments of temporal order, simultaneity and duration are inconsistent. Iperception. 2014;5: 559–571.

39. Machulla T-K, Di Luca M, Ernst MO. The consistency of crossmodal synchrony perception across the visual, auditory, and tactile senses. J Exp Psychol Hum Percept Perform. 2016;42: 1026–1038.